All-electron local-density-functional theory of alkali-metal adsorption on transition-metal surfaces: Cs on Mo(001)

S. R. Chubb,* E. Wimmer,† and A. J. Freeman
Department of Physics and Astronomy and Materials Research Center, Northwestern University, Evanston, Illinois 60208

J. R. Hiskes and A. M. Karo
Lawrence Livermore National Laboratory, Livermore, California 94550
(Received 7 November 1986; revised manuscript received 16 April 1987)

The electronic structure of a clean Mo(001) surface and the bonding between a dense [$c(2\times2)$] Cs overlayer with the Mo(001) substrate are studied using all-electron local-density-functional theory and the full-potential linearized augmented-plane-wave (FLAPW) method for thin films. We find that Cs(s)-Mo(d) interactions lead to a shift of the high-lying surface state at $\bar{\Gamma}$ from 0.1 to 0.9 eV below the Fermi level and to a Cs(s)-Mo(d) band with an upward dispersion away from $\bar{\Gamma}$. Furthermore, Cs(d)-Mo(d) interactions reduce the high Mo-surface-projected density of states at E_F by shifting some of the Mo(d) bands [notably those midway between $\bar{\Gamma}$ and M of the Mo(001) surface Brillouin zone] to larger binding energies. In addition, Cs is found to induce unoccupied adsorbate-surface states of Cs p and d character, located 0.8 eV above the Fermi level. Similar to the case of tungsten metal, the lowering of the work function of Mo(001) due to Cs adsorption is explained by the formation of multiple surface dipoles involving a polarization of the Cs $6s$-derived states towards the transition metal and a counterpolarization of the Cs $5p$ states.

I. INTRODUCTION

In search of efficient negative H^- and D^- sources as needed in thermonuclear fusion devices, experimental and theoretical efforts have concentrated on cesiated transition-metal surfaces such as those of tungsten and molybdenum. These systems are characterized by low work functions, low H and D sticking coefficients, and high yields of backscattered[1,2] and sputtered[3] negative ions.

In a recent theoretical study,[4] the electronic structure of a Cs monolayer on a W(001) surface (Cs/W) has been investigated using the all-electron local-density-functional (LDF) approach. From this study,[4] we have obtained a detailed description of the interaction between the alkali-metal adsorbate and the transition-metal substrate (in the high-coverage limit); the Cs $6s$-derived, widely extended valence electrons are polarized towards the transition-metal surface, which is dominated by localized W d electrons, forming partly covalent bonds with the Cs states. This leads to an increase of electronic charge between the adsorbed Cs atoms and the W atoms in the surface layer. As a response to this polarization of the Cs $6s$-derived valence states, the Cs $5p$ semicore electrons are markedly counterpolarized, which leads to an increase of electronic charge immediately above each Cs atom. As a consequence, two dipoles are formed which are centered around the plane of the Cs atoms. The competition between these polarized distributions of charge leads to a positive increase in the average value of the single-particle potential, which in turn results in a lowering of the work function. Furthermore, as a consequence of Cs adsorption, the W(001) surface state, located at $\bar{\Gamma}$ 0.3 eV below the Fermi level, is shifted by about 1 eV to larger binding energy due to the formation of a polarized covalent bond with the Cs $6s$-derived valence states. This theoretical prediction[4] has been found independently and confirmed by angle-resolved ultraviolet photoemission experiments.[5,6]

The aim of the present work is to extend the theoretical studies of alkali-metal adsorption on transition-metal surfaces to the system Cs on Mo(001) (Cs/Mo) and to deepen the analysis by making use of more detailed representations such as two-dimensional (2D) energy-band structures as well as energy-resolved density and density-difference plots. Since the electronic structure of Cs adsorbed on Mo and W are very similar, many of the insights gained from the present, more detailed study also apply to Cs/W.

The isoelectronic bulk systems Mo and W and their (001) surfaces differ in subtle ways: (i) the bulk bcc lattice constant of W is only slightly (0.3%) larger (despite the fact that the atomic number of W is almost twice as large as that of Mo); (ii) in the free atoms, the Mo $4d$ level is about 0.5 eV below the Mo $5s$ level, while the ordering of the corresponding levels in W is reversed, and the atomic W $5d$ level is about 1.5 eV above the W $6s$ level; the Mo $4d$ orbitals are slightly more contracted than the corresponding W $5d$ states; (iii) the width of the occupied bulk Mo bands[7] is 6.5 eV, while the corresponding value for bulk W (Ref. 8) is 9.7 eV; and (iv) both the Mo(001) and the W(001) surfaces have similar surface states,[6] and both surfaces reconstruct below room temperature into a $c(2\times2)$ structure with nearly equal vectors of reconstruction; $(\pi/a,\pi/a)$ for W(001); $(0.9,0.9)\pi/a$ for Mo(001) (Ref. 9) with a being the cubic lattice constant.

The crystallographic structures of the Mo(001) surface with increasing Cs coverages have been investigated by re-

cent studies using low-energy electron diffraction (LEED) and Auger electron spectroscopy (AES);[10] at a Cs coverage of 0.3 monolayers (the completed monolayer occurs at $\Theta=0.43$), the adsorbate induces a $(\sqrt{2}\times\sqrt{2})R45°$ reconstruction of the substrate; at $\Theta=0.25$, Cs forms an ordered $p(2\times2)$ overlayer structure without a substrate reconstruction.[10] Analogous to the Cs/W(001) system,[10] the minimum in the work function occurs for the $p(2\times2)$ Cs coverage where the work function is lowered[11,12] by 3.54 eV with respect to the clean Mo(001) surface. For $p(2\times2)$ Cs/W(001) the corresponding work-function lowering is 3.04 eV.[13] For up to 0.7 monolayers of Cs on Mo(001), Riwan *et al.*[10] observed a contraction of the $p(2\times2)$ overlayer along the [110] direction resulting in a quasihexagonal structure for $0.3<\Theta<0.43$ and a true hexagonal structure at monolayer coverage ($\Theta=0.43$). Furthermore, at this coverage a $(\sqrt{2}\times\sqrt{2})R45°$ adsorbate-induced reconstruction of the Mo substrate has been deduced.[10] Despite this diversity in overlayer structures, the overall electronic structure of this system (as manifested by work-function changes,[12] photoemission spectra, and energy-loss spectra[6]) exhibits a smooth dependence with respect to Cs coverage and, remarkably, is rather insensitive to the observed adsorbate-induced reconstruction of the substrate. (The Cs-induced reconstruction is presumably different from that of the clean surface.) This finding suggests only weak dependence of the electronic structure on the actual lateral position of the Cs adatoms. Thus, in the present work, the completed Cs monolayer has been modeled by a $c(2\times2)$ overlayer structure,[4] resulting in a substantial reduction in computational effort, but without significant loss of information concerning the interaction between the adatoms and the substrate. In fact, our model exhibits the same nearest-neighbor geometry as in the $p(2\times2)$ coverage, where Cs is adsorbed in fourfold hollow sites and the substrate is unreconstructed.

In the next section (II), we review various details associated with the method of the calculation. In Sec. III, we discuss our results. In Sec. IV, we give a summary of our findings and conclusions.

II. COMPUTATIONAL ASPECTS

The Mo(001) substrate (cf. Fig. 1) is represented by a five-layer slab using the bulk lattice constant of 3.147 Å (5.9475 a.u.). The surface layer is assumed to be unrelaxed and unreconstructed. The Cs overlayer is modeled by a $c(2\times2)$ structure (on both sides of the Mo slab) resulting in two surface Mo atoms per adsorbed Cs atom. The plane of the Cs overlayer atoms is chosen to be 2.9 Å (5.48 a.u.) above the plane of the surface Mo atoms as in Ref. 4.

The electronic structures of the clean Mo(001) surface, the cesiated surface, and an unsupported Cs monolayer are calculated with the full-potential linearized augmented-plane-wave (FLAPW) method[14,15] for thin films using the Wigner exchange-correlation potential[16] in the local-density-functional (LDF) single-particle equations.[17,18] All electrons are treated self-consistently; the core electrons fully relativistically within a central field approximation, and the valence electrons, including the Cs 5*p* electrons, semirelativistically,[19] i.e., by dropping the spin-orbit–interaction term but retaining the other relativistic terms in the effective single-particle Hamiltonian. The single-particle wave functions for the valence states are expanded variationally in linearized augmented plane waves with a maximum value for Rk of 7.2 (R is the muffin-tin radius of the Mo spheres with a value of 2.5496 a.u.). With this choice we obtain about 70 basis functions per atom. Inside the muffin-tin spheres, angular momentum components up to $l=8$ are included in the augmentation of the wave functions. In the matrix elements of the Hamiltonian, contributions from the full potential

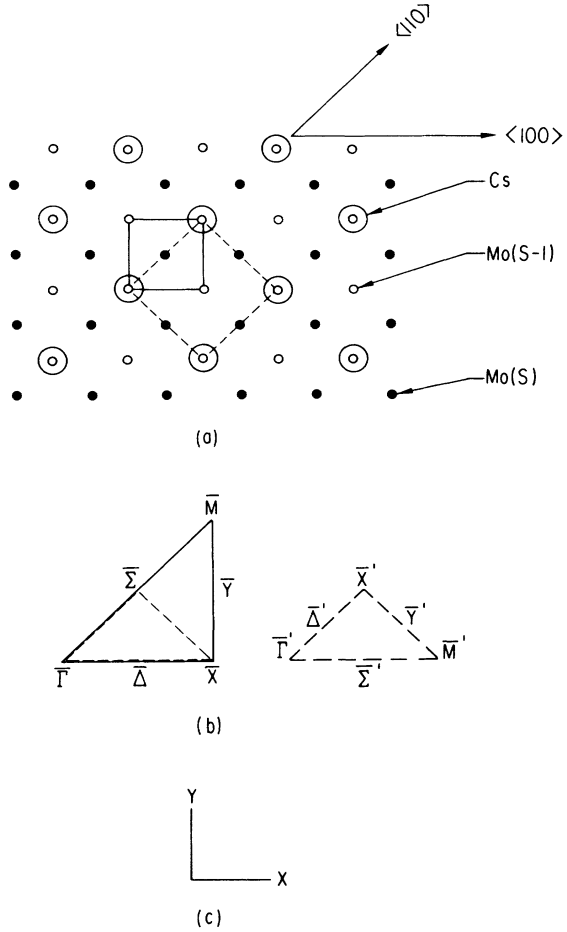

FIG. 1. (a) Structure of $c(2\times2)$ Cs on Mo(001); the two-dimensional unit cells of the clean (solid lines) and cesiated (dashed lines) substrates are rotated by 45° relative to each other. Mo(S) denotes the surface Mo atom; Cs and Mo (S-1) label the Cs and first subsurface Mo atoms, respectively. (b) The irreducible wedge of the first surface Brillouin zone for the clean (001) surface (solid lines, left-hand side) and for the $c(2\times2)$ structure (dashed lines); symmetry points and lines in the $c(2\times2)$ structure, throughout, are distinguished from those in the clean surface by primes. (c) The in-plane–coordinate axes of the clean surface which are used throughout in the designation of all angular momentum components of individual states.

(i.e., a potential without any shape approximations) are calculated rigorously. The mirror (z-reflection) symmetry with respect to the central plane of the film is used to divide the secular matrix into two blocks, which allows us to compute the resulting even ($+$) and odd ($-$) states separately.

Eigenvalues and wave functions are computed at 21 and 19 k points in the irreducible part of the two-dimensional surface Brillouin zones (BZ's) of the clean and cesiated Mo(001) surfaces, respectively. Fermi energies, charge densities, and densities of states are constructed from this k mesh by applying the Wang-Freeman triangular-integration scheme.[20] This scheme also is used to evaluate the local density of states $g(r,E)$, in particular for $E=E_F$.

In the interstitial region this charge density is expanded in a symmetrized Fourier (star-function) representation using reciprocal lattice vectors, G, up to a maximum RG value of 16 (again, R is the Mo muffin-tin radius) resulting in 880 three-dimensional star functions. In the "vacuum region," which is defined to begin at 2.612 a.u. above the plane of the surface atoms for the clean Mo(001) surface and 3.622 a.u. above the plane of the adsorbed Cs atoms for Cs/Mo(001), 13 two-dimensional star functions are used to describe the warping of the charge density. At distances greater than 10 a.u. above the vacuum boundary, these warping contributions become negligible and are neglected. The remaining star-function contributions to the density, which vary only in the direction normal to the surface, are evaluated in planes extending out to 25 a.u. away from the vacuum boundary. Inside the muffin-tin spheres the charge density is represented by an expansion in spherical harmonics including components up to $l=8$. Across the interstitial-vacuum boundary the continuity of the charge density is better than 0.01% and across the sphere-interstitial boundaries better than 0.3%.

Poisson's equation for this full charge density is solved as described earlier,[21] and the Wigner interpolation form[16] of correlation is used with $\alpha t^{1/3}$ ($\alpha=2/3$, $t=81/\pi n$, n is the electron density) exchange in the exchange-correlation potential. This last quantity is obtained by least-squares-fitting techniques with a root-mean-square deviation of better than 1 mRy. The effective potential is represented by the same analytic expansions as the charge density described above. The convergence of the charge density to self-consistency was achieved by alternating between a straight mix between the input and output densities (typically using 3–5 % of the output densities) and a mixing scheme of Anderson[22] as suggested by Hamann.[22] A total of about 50 iterations was necessary to converge the average rms difference between input and output densities to less than 2×10^{-4} e/(a.u.).[3] This corresponds to an average rms difference between the input and output potentials of about 10 mRy. It should be emphasized, however, that due to the overshooting of the output potentials, the eigenvalues, which are calculated from the input potentials, are converged to about 1 mRy.

The density-of-states plots are calculated from the FLAPW eigenvalues by a triangular interpolation technique[20] and a broadening by Gaussians with a full width at half maximum of 0.1 eV. The energy-band structure plots are obtained by spline interpolations of FLAPW eigenvalues calculated for 15 k points on each of the three symmetry lines of the irreducible parts of the surface BZ's. The square of the amplitudes of the single-particle wave functions, integrated over muffin-tin spheres, serves as a guideline to detect localization in the surface layers.

III. RESULTS AND DISCUSSION

A. Densities of states

1. *Clean Mo(001) and unsupported Cs monolayer*

The local density of states (LDOS) for the central and subsurface (S-1) atoms in the five-layer Mo(001) film exhibit the main features of the DOS of bulk Mo (Ref. 7) as indicated in Fig. 2. In particular, we find a pronounced minimum 0.5 eV below E_F, which is characteristic for bcc transition metals.

The most striking difference between the surface LDOS and the bulklike DOS in the interior of the film is the existence of a single, sharp peak just at E_F in the surface layer. In addition, pronounced surface-induced peaks are found at energies of -0.07 and -1.1 eV. In the surface LDOS, the bulk features which contain significant s contributions at the bottom of the d band between -5 and -3.7 eV are markedly reduced. The LDOS of the vacuum region, though rather small (note the scale in Fig. 2), provides a convenient representation of the amount by which surface states project out into the vacuum. In the occupied part of the LDOS, the largest contributions to the "vacuum" LDOS originate from states at the Fermi energy. Further contributions are found at -0.7 and -3.6 eV. The unoccupied states at 1.2 eV above the Fermi level exhibit a relatively large vacuum LDOS.

The interstitial LDOS (Fig. 2) reproduces the main features of the total DOS, discussed later, and the small differences reflect the varying degree of localization and the wave functions inside the muffin-tin spheres. A striking feature is the relatively large interstitial contribution of states at -3.5 eV, demonstrating a significant free-electron-like (s-like) character, as can also be seen from the angular-momentum projection inside the spheres. As a matter of fact, states at -3.5 eV are found to have a large s-like amplitude in the surface Mo atoms and give rise to a little peak in the vacuum LDOS.

The local density of states for the unsupported Cs monolayer (shown in Fig. 3) reveals that the Cs 6s monolayer band, which possesses an occupied width of 1.5 eV, begins to hybridize with the unoccupied 6p and 5d bands at about -0.25 eV, below the Fermi energy (which is 2.36 eV below the vacuum zero). At the Fermi level, the degree of this hybridization has intensified to the point that essentially equal contributions from p, d, and s-like electrons are present. The four unoccupied peaks above E_F begin as a continuation of this strongly hybridized band with a marked attenuation of s character beginning 0.3 eV above E_F, followed by p-electron attenuation at 1 eV above E_F. Thus, relatively large p and d contributions are present in the Cs band at and immediately above E_F.

Also present (but not shown in Fig. 3) in the Cs monolayer LDOS are the semicore $5p$ electrons at -10 eV. These "bands" are essentially localized inside the Cs muffin tin, with approximately 4% of the corresponding charge located in the interstitial and vacuum regions, and have a nontrivial width (0.7 eV). The positions, shape, and width of these $5p$ peaks are readily identified in Fig. 4, which shows the total densities of states of Cs, Mo, and Cs/Mo.

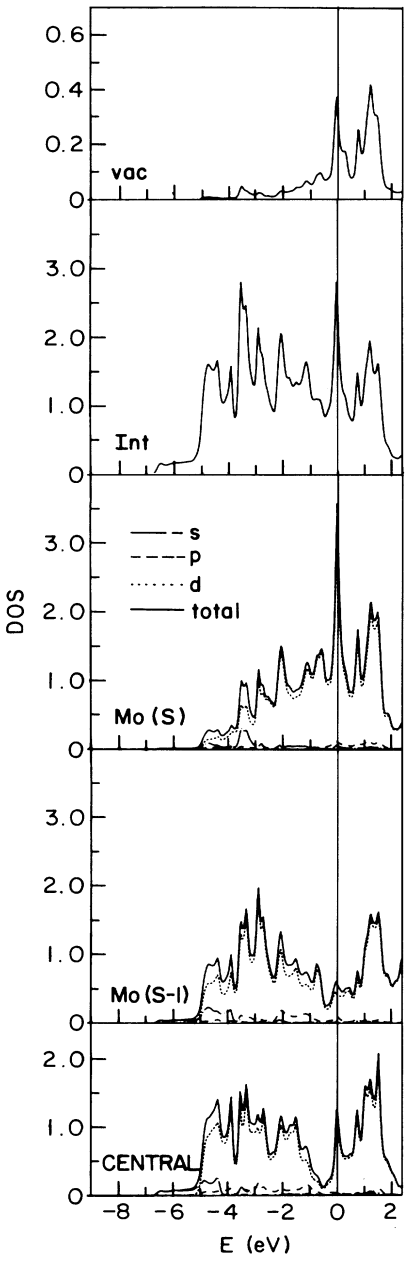

FIG. 2. The local density of states (DOS, referred to as LDOS in the text) for the clean-Mo-substrate vacuum (vac) and interstitial (int) regions (in states/eV unit cell), and inequivalent muffin-tin sphere regions [Mo(S), Mo(S-1), central] in units of states/eV atom; central refers to the muffin tin located in the central layer of the five-layer film. The index for the symbols used in the angular momentum decomposition inside each muffin tin is shown in the middle of the figure.

2. *Cesiated Mo(001)*

As expected, the largest Cs-induced changes in the LDOS's are found in the Mo atoms at the surface (Fig. 5). The single peak at E_F in the surface LDOS obtained for clean Mo(001) is reduced upon cesiation and new peaks (labeled A and B in Fig. 5) are induced at -0.9 and -0.2 eV. The LDOS of the Cs sphere (Fig. 5) shows a predominantly s-like peak at -0.9 eV. Immediately above this resonance, a strong hybridization with d-like and p-like components occurs, similar in character to the unsupported Cs monolayer (cf. Fig. 3). But in contrast to the unsupported monolayer, the Cs d-like DOS now extends further into the occupied states. Associated with the Cs s resonance we find at the same energy a sharp d resonance for the surface Mo atoms, a sharp peak in the interstitial LDOS, and a little peak in the vacuum LDOS (cf. Fig. 5). These structures (peak A in Fig. 5) can be interpreted as evidence for Cs(s)-Mo(d) bonding. Furthermore, associated with the predominantly Cs d-like peak centered at -0.2 eV (cf. Fig. 3) we find a d resonance in the surface Mo atoms with noticeable p admixture. Corresponding

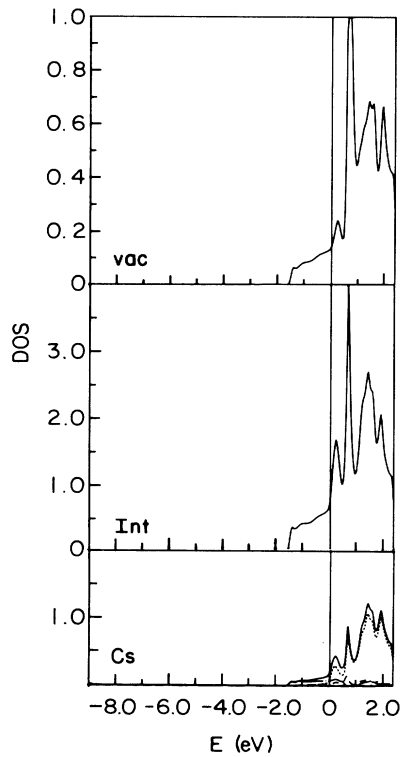

FIG. 3. The local density of states (DOS, referred to as LDOS in the text) of the free-standing Cs monolayer; labels vac and int are defined as in Fig. 2; the decomposition by angular momentum components inside the Cs muffin tin (denoted by Cs, as in Fig. 1) is shown as in Fig. 2. Units of DOS are as in Fig. 2.

structures at −0.2 eV are present in the LDOS's of the interstitial and vacuum regions. These features (peak *B* in Fig. 5) of the LDOS's provide evidence for a significant Cs(*d*)-Mo(*d*) component to the Cs—Mo bonding. Further substantion of this *d*-bonding feature is provided by Fig. 6, which shows the integral of the difference between the total densities of states of the cesiated and clean substrates. Essentially, this plot shows the energetic distribution of the Cs valence electrons after chemisorption. In the occupied region of this plot, the greatest change in the number of states occurs between −0.4 eV and E_F, and the maximum of the resulting peak occurs at precisely the point (−0.2 eV) where the LDOS of the cesium sphere has its maximal *d* charge. Furthermore, after achieving a maximum at −0.2 eV, the number of states declines by almost 0.4 electrons, indicating a significant loss of states from the Mo substrate between −0.2 eV and E_F, and a strong Cs(*d*)-Mo(*d*) hybridization. The *sp*-like Mo states at −3.5 eV give rise to only a very weak resonance within the Cs sphere.

Cesiation causes the Cs monolayer 5*p* semicore states to be shifted by approximately 0.5 eV to lower binding energies (Fig. 4) but does not affect the shape of the corresponding peak in the DOS. As expected, these states are mainly localized within the Cs spheres, but show a significant peak in the interstitial LDOS and a small peak in the vacuum LDOS.

In the unoccupied part of the DOS, the presence of Cs *d*-like states changes the peak structure to a large extent, as can be seen from the total DOS's of the clean

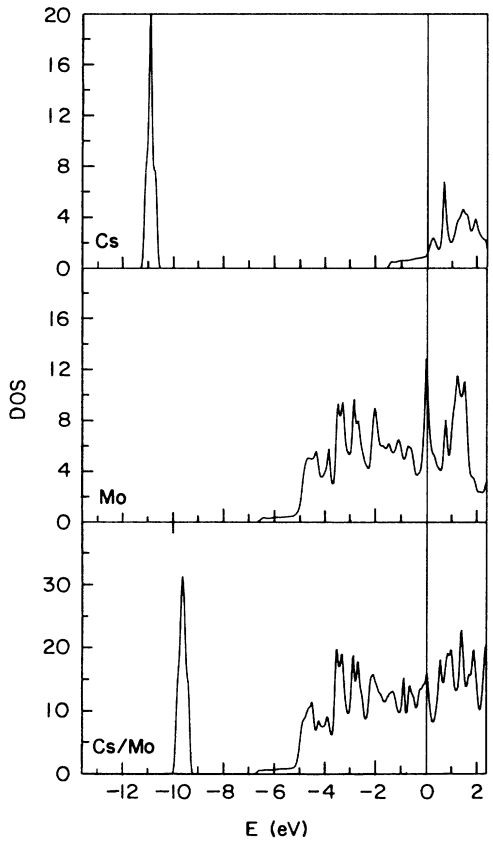

FIG. 4. The total DOS's for the free-standing Cs monolayer (Cs), clean five-layer Mo substrate (Mo), and cesiated substrate (Cs/Mo); the vertical scale (in units of states/eV unit cell) for Cs/Mo has been doubled because there are twice as many Cs and Mo states in the $c(2\times2)$ unit cell.

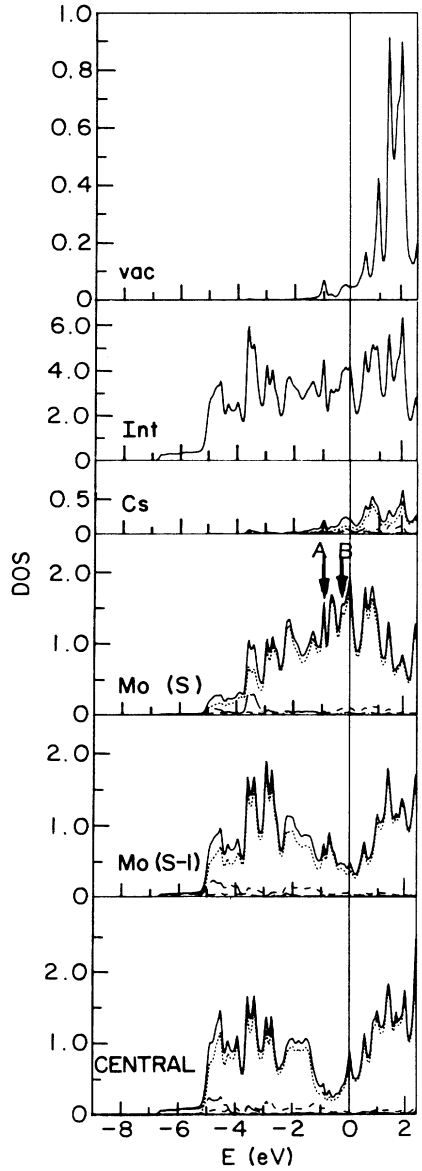

FIG. 5. The local density of states (DOS, referred to as LDOS in the text) of $c(2\times2)$ Cs adsorbed on Mo(001); vac, int, Cs, Mo(*S*), Mo(*S*-1), and central are defined as in Figs. 2, 3; Mo(*S*-1) refers to the muffin-tin sphere located directly below the Cs and has a LDOS essentially indistinguishable from the remaining Mo(*S*-1) muffin-tin sphere. The positions of the two new peaks in the Mo(*S*) sphere (alluded to in the text) at −0.2 and −0.9 eV are labeled *A* and *B*. Units of the DOS are as in Fig. 2.

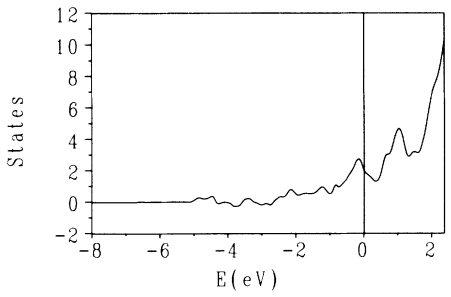

FIG. 6. The integral I (in states/unit cell, normalized to the Cs/Mo cell) of the difference between the total DOS of Cs/Mo and superposition of the total DOS's of the clean Mo substrate and free-standing Cs monolayer.

(Fig. 2) and cesiated (Fig. 4) slabs, as well as from the plot of the integrated difference of DOS's (Fig. 6). This last plot shows a gain of almost seven states between 1.8 eV and the vacuum zero, which is precisely the region where the clean Mo substrate obtains its minimal unoccupied region DOS.

Specifically, at an energy of 0.3 eV above the Fermi level we find a pronounced double-peak structure of Cs d and Mo d character. This adsorbate-induced peak should be observable by inverse photoemission spectroscopy.

B. Energy-band structure

The energy bands discussed below provide a guideline for the interpretation of experimental data near the $p(2\times2)$ coverage where the local Cs-Mo coordination is the same as in the present calculation, i.e., with Cs adsorbed in fourfold hollow sites and no reconstruction of the substrate. Thus, the focus here is on the Cs-Mo interaction.

The energy-band structures of the five-layer Mo(001) slab with $c(2\times2)$ Cs overlayers (on both sides) are presented in Fig. 7 in the inner panels. Surface states (SS's) and surface-resonance (SR) states are marked by bold lines. For comparison with the clean surface,[23,24] the backfolded bands [involving the specific boundary lines, $\bar{\Gamma}'$-$\bar{M}'$ and $\bar{X}'$-$\bar{M}'$, of the $c(2\times2)$ surface BZ, which is shown by dashed lines in Fig. 1(b)] are plotted in the outer panels of Fig. 7.

The Cs adsorption (cf. Fig. 7) causes only very subtle changes in the occupied part of the energy-band structure with the largest effects occurring near the center of the BZ, $\bar{\Gamma}'$, and near symmetry point $\bar{X}'$ [$=\frac{1}{2}(\bar{\Gamma}\bar{M})$ in the Mo(001) BZ]. In the occupied region, away from $\bar{\Gamma}'$, with the exception of two pairs of SS's at $\bar{X}'_1$ (which will be discussed below), these changes result entirely from avoided crossings which develop as a consequence of the reduced symmetry of the adsorbate environment. In the unoccupied region, most of the changes are accounted for in a similar manner. Additional modification of the bands above E_F, however, does occur due to the presence of Cs d states (as discussed below).

At $\bar{\Gamma}'$, the bottom of the Cs s-like valence band interacts with the substrate to form polarized covalent bonds of Cs(s) and Mo(d) character. This adsorbate-substrate interaction causes the high-lying SS at $\bar{\Gamma}'$ to be shifted by 0.9 eV to larger binding energies. An analogous shift of 1.0 eV has been obtained theoretically for the cesiated W(001) surface[4,5] and has been confirmed by independent angle-resolved ultraviolet photoemission experiments for both the W(001) and Mo(001) surfaces.[4,5] A combined experimental and theoretical study of these Cs-induced shifts of the high-lying SS's at $\bar{\Gamma}'$ of the (001) faces of W, Mo, and Ta has been presented earlier.[6]

The positions of all of the remaining occupied bands at $\bar{\Gamma}'$ (shown in Fig. 7) are almost identical for Cs/Mo and Mo. Here, we find even (+) and odd (−) pairs of degenerate $d_{xz,yz}$-like SR states at −0.04 (−0.04) eV and −2.04 (−2.09) eV, of $d_{3z^2-r^2}$-like singlet resonances at −2.28 (−2.35) eV and −2.85 (−2.91) eV, and of $d_{x^2-y^2}$-like singlet SR's at −2.34 (−2.34) eV and −0.51 (−0.52) eV for Mo (Cs/Mo).

In the unoccupied region, immediately above E_F, a new surface state appears at $\bar{\Gamma}'$ with energy 0.80 eV (split by 0.08 eV due to film-thickness effects). This unoccupied state, which is d_{xy}-like (relative to the coordinate system of the clean surface), is the remnant of the resonance from the $\bar{\Delta}_2$ line in the unfolded [Mo(001)] structure. This state undergoes a pronounced anticrossing along the $\bar{\Sigma}'_2$ line with the d_{xy}-like state from the $\bar{Y}_2$ line. As a consequence, in the folded bands (Fig. 7), where the crossing is allowed, these SR's do not hybridize and pass very near each other at $\bar{\Gamma}'_2$, where their energies are 1.43 and 1.31 eV, while level repulsion causes them to separate by 0.5 eV at the zone center in the cesiated structure.

Between the position of the avoided crossing ($\sim0.2\bar{\Gamma}'_2$–$\bar{M}'_2$) and $\bar{\Gamma}'_2$, the lower SR state is extremely flat, and its energy at the near crossing is also ~0.8 eV. This energy also corresponds to the position of the first shoulder in the first peak above E_F in the integrated DOS difference (Fig. 6), and is the location of maximal unoccupied Cs d charge (Fig. 5). These facts imply significant Mo(d)-Cs(d) hybridization. Furthermore, this avoided crossing is far more accentuated than the other anticrossings and occurs in the type-2 bands, where hybridization involving nearly-free-electron (p_z-, s-, and $d_{3z^2-r^2}$-like) states is forbidden. In addition, at $\bar{\Gamma}'_2$, this unoccupied state possesses large Cs d_{xy}-like charge. These observations imply that this state has evolved from significant interaction between localized ($d_{xz,yz}$- and d_{xy}-like) states on the Mo(S) and Cs layers. At $\bar{\Gamma}'_2$, quite astonishingly, we find that this hybridization is entirely Mo(d_{xy})-Cs(d_{xy})-like.

Immediately above this new, unoccupied surface state, there is a second SS, which is not present in the backfolded bands. It appears at $\bar{\Gamma}'_1$ with energy 1.04 eV [1.02 (1.06) eV for the corresponding (+) (−) partner states]. This type-1 SS develops at the first maximum above E_F as shown in Fig. 6. Here, the Cs charge is predominantly p_z-like. The band can be viewed as the remnant of the first excited state of the isolated Cs monolayer (which in various geometries, hexagonal,[25] square,[26] involving a compa-

rable lattice spacing, is 6p-like). Furthermore, it has been suggested recently[5] that the gradual shift of the main peak of the electron-energy loss spectra[4] with increasing Cs coverage can be accounted for by an interband transition between the high-lying SS band and this unoccupied p_z band.

As we pointed out in our discussion of the SS located at 0.8 eV, the SR character from the d_{xy}-like (Mo) states at 1.31 and 1.43 eV has been shifted to the new SS found at 0.80 eV and the SR at 1.35 eV. The remaining SR band [whose (+) (−) partners have energies 1.90(2.94) eV], which is $p_{x,y}$-$d_{xz,yz}$-like, originates from the (unfolded) $\bar{M}$ point, and possesses a large vacuum component, hybridizes with the Mo $d_{xz,yz}$-like bands from $\bar{\Gamma}'$ (which possess energy 1.4 eV in the clean film), causing this last set of states to be lowered by 0.05 eV. In addition, the remaining resonance hybridizes with Cs(d) states, which achieve a local maximum in the Cs LDOS (Fig. 5) at 2 eV. As a consequence, level repulsion pushes these states above the vacuum zero.

Summarizing, we find that the most important changes in the occupied part of the band structure occur at $\bar{\Gamma}'$. Here, the high-lying SS is shifted downward by 0.9 eV, while the position of the low-lying SS does not change. Away from $\bar{\Gamma}'$, most of the changes in the band structures are minor and result from the reduced symmetry of the adsorbate environment. At $\bar{X}'_1$, Mo d states just below E_F are shifted to larger binding energies by about 0.2 eV due to hybridization with Cs d states, giving rise to peak B in the LDOS shown in Fig. 5. Because of the avoided crossings of bands [originating from the symmetry lines, $\bar{\Gamma}$-$\frac{1}{2}d$($\bar{\Gamma}\bar{M}$), and $\bar{M}$-$\frac{1}{2}$($\bar{\Gamma}\bar{M}$) in the unfolded Mo structure] which are induced by the adsorption, these last two pairs of surface states are split by about 0.1 eV. Also, ad-

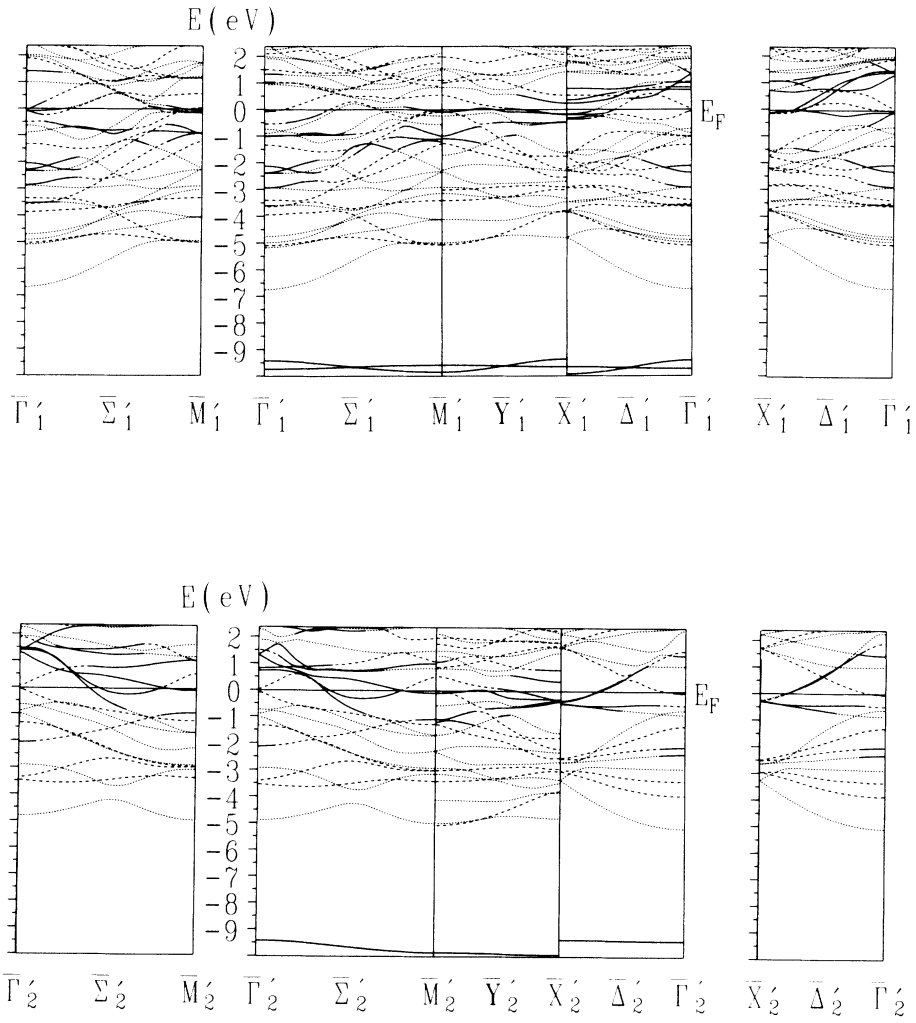

FIG. 7. Energy bands, SS's, and SR states of the cesiated film (inner panels) and folded bands from the clean substrate (outer panels), along the boundary of the BZ [shown on the right hand side of Fig. 1(b)]; upper and lower portions of the figure correspond to even (1) and odd (2) states. Dotted and dashed lines correspond to even (+) and odd (−) states. Solid lines designate states which possess more than 60% of their charge in the Mo(S) or Cs muffin-tin spheres in the case of Cs/Mo (inner panels) and 60% of their charge in the Mo(S) sphere in the case of the folded bands of the clean surface (outer panels).

ditional surface character is transferred to each odd (−) member of each pair. Thus, the adsorption leads to an enhancement of the surface character and stabilization of the SS's located immediately below E_F near the $\bar{X}_1'$ point. The changes along the $\bar{\Sigma}_2'$ line imply important Mo(d)-Cs(d) interaction just above E_F, involving a large Cs(d_{xy}) component. We have already identified evidence for a large component of Cs d electrons near E_F in the discussion of the LDOS's (Fig. 5). In the next section, we will see additional evidence of Mo(d)-Cs(d) interaction among occupied states near E_F.

C. Energy-dependent electron densities

An energy-dependent electron density (or "local" density of states) can be defined by

$$n(r,E)=2(4\pi^2)^{-1}\int_{\mathrm{BZ}}\sum_i |\psi_i(r)|^2\delta(\epsilon_i(k_\parallel)-E)d^2k_\parallel \quad (1)$$

which is related to the usual density of states by

$$g(E)=\int_{\Omega_F} N(r,E)d^3r \ ,$$

where Ω_F denotes the film unit cell and the factor of 2 in Eq. (1) is present to account for the spin degeneracy. This energy-dependent electron density, $n(r,E)$, is of particular interest at $E=E_F$.

As stated in the discussion of the densities of states, cesiation of the Mo(001) surface causes a reduction of states at the Fermi level. Figure 11 reveals the nature of the Cs-induced redistribution of charge at E_F. On the clean Mo(001) surface [cf. Fig. 8(a)], we see in the surface and, to a lesser extent, also in the central layer, the prevalence of d_{xy}-like states. The orbitals of the SS's and SR states show, as expected, their largest amplitude near the sites of the surface atoms and couple more strongly with the atoms directly underneath (i.e., the atoms in the center of the five-layer film) than with the subsurface atoms, which exhibit more bulklike behavior in the sense that their DOS at the Fermi level is small. Furthermore, Fig. 8(a) reveals that there is a significant $d_{3z^2-r^2}$-like orbital-character coupling atoms in the central and surface layers. In the vacuum region above the surface atoms, $n(r,E_F)$ [Fig. 8(a)] becomes planar at about half a lattice spacing away from the surface atoms.

As Cs is deposited onto the Mo(001) surface, $n(r,E)$ (shown in Fig. 8) changes substantially: the $d_{3z^2-r^2}$-like orbitals of the surface and central layer atoms are removed and the d_{xy}-like orbitals become more apparent. The density near the Cs atoms exhibits a mixture of s, p, and significant d character. In fact, we find noticeable $dd\sigma$ contributions to the bonding between Cs and Mo. There is a significant electron density between adjacent Cs atoms which indicates a metallic character of the Cs overlayer. Above the Cs atoms, $n(r,E)$ decays more slowly into the vacuum than in the case of the clean surface.

D. Charge-density differences

Cesiation causes a strong hybridization between the Cs 6s valence electrons and the localized $d_{3z^2-r^2}$-like electrons from the surface layer of the Mo substrate. We have already examined various results of this effect: (a) the shift of the Mo surface [Mo(S)] LDOS peak at E_F to greater binding energies, (b) a shift of Mo states with an associated charge of approximately 0.4 electrons from E_F to energies less than −0.2 eV, and (c) the shift of the high-lying SS at $\bar{\Gamma}$ from −0.1 to −1 eV. Most importantly, this hybridization leads to a significant build up of charge in the region between Mo(S) and the Cs overlayer and a loss of charge from the region immediately above each Mo surface atom (cf. Fig. 9).

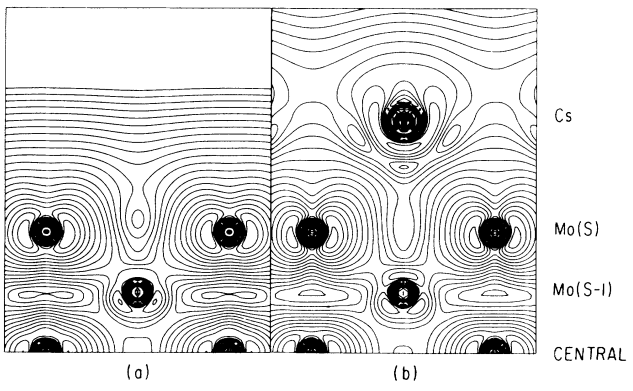

FIG. 8. The valence electron density at E_F for the clean (a) and cesiated (b) Mo substrate; contours are shown in the (110) plane logarithmically incremented by factors of $\sqrt{2}$. The smallest contour in (a) is 0.001 e/bohr^3; in (b) the smallest contour is 0.002 e/bohr^3.

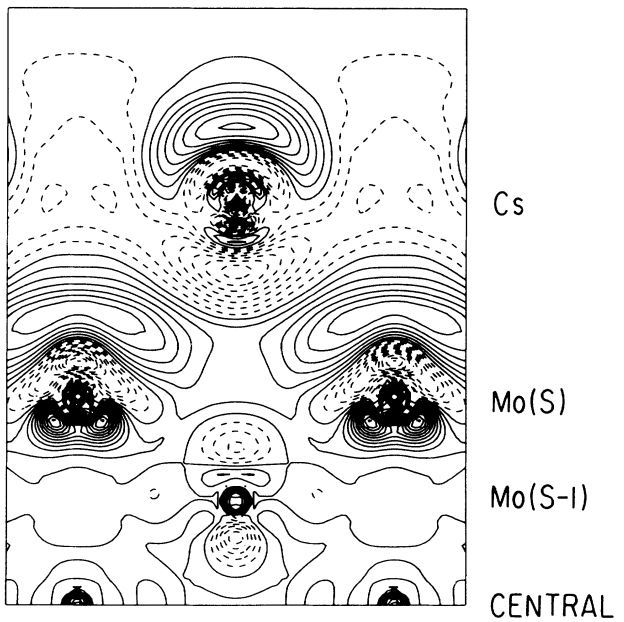

FIG. 9. Difference between total densities of Cs/Mo and the superposition of Mo and Cs; contours are linearly spaced in increments of 0.0005 e/bohr^3 and are shown in the same plane as in Fig. 8; non-negative and negative values of the density are shown by solid and dashed contours, respectively.

Figure 9 shows the difference of the total charge densities in the (110) plane between Cs/Mo(001) and the superposition of the Cs monolayer and Mo(001) substrate. As in Cs/W(001) (Ref. 4), cesiation causes $5p$ charge to be redistributed both above the Cs atom and into the region immediately above the Mo(S) atoms. Thus, as in the earlier study of Cs/W(001), the rearrangement of the Cs $5p$ electrons involves a net gain in electronic charge above the Cs atoms and a depletion of charge immediately below the Cs.

Figure 10 further quantifies this $5p$ polarization. Here, the difference between the semicore-valence charge densities of Cs/Mo and the Cs monolayer is plotted. In order to monitor more clearly the rearrangement of $5p$ electrons near the core, spherically symmetric contributions from inside the Cs muffin tin in both densities have been suppressed. Contours in this plot are logarithmically spaced. The figure provides evidence for a strong polarization of the localized Cs semicore electrons away from the Mo substrate. This counterpolarization of $5p$ electrons leads to the depletion of charge immediately below the Cs atom. On the other hand, the figure shows that the tails of these semicore electrons both above and below the Cs atoms are attracted towards the Mo substrate. In addition, Fig. 9 reveals a depletion of charge immediately above and below the subsurface Mo atoms which is not present[4] for W.

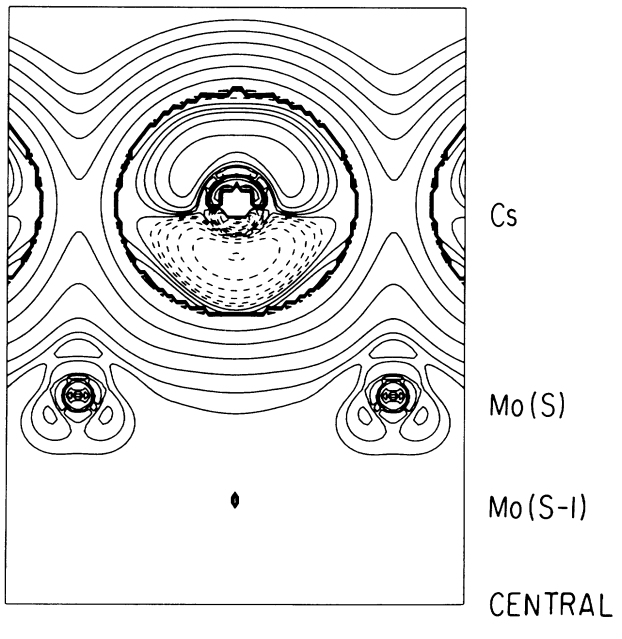

FIG. 10. Difference between the $5p$ semicore densities of Cs/Mo and Cs; all spherically symmetric contributions have been suppressed. Contours are logarithmically incremented by a factor of 2, with positive values between 0.0001 and 0.0008 e/bohr^3, and negative values between -0.0001 and -0.0032 e/bohr^3. Non-negative and negative values are shown by solid and dashed contours, respectively.

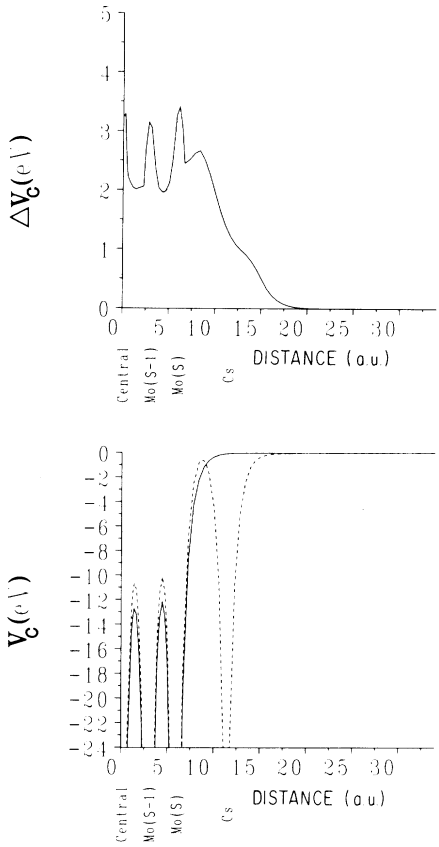

FIG. 11. (a) Difference between planar-averaged Coulomb potentials $V^{Cs/Mo} - V^{Mo} - V^{Cs}$ vs distance above the central layer; (b) planar-averaged Coulomb potentials of the clean (V^{Mo}, shown by solid lines) and cesiated ($V^{Cs/Mo}$, shown by dashes) substrates.

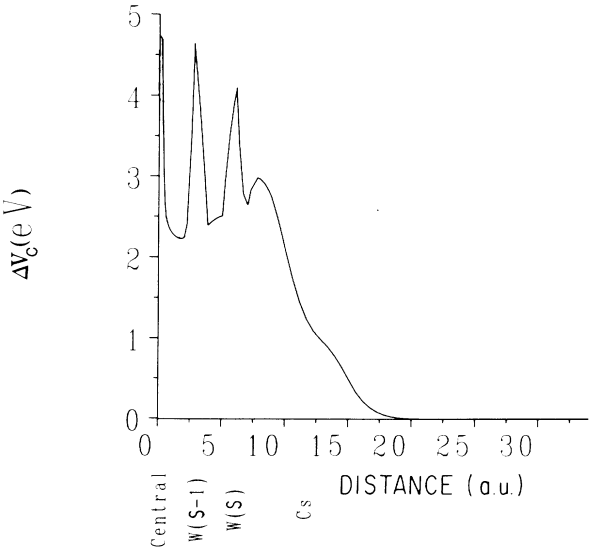

FIG. 12. Difference between planar-averaged Coulomb potentials, as in Fig. 11(a), for W(001): $V^{Cs/W} - V^{W} - V^{Cs}$.

E. Work-function lowering

The important charge rearrangement at the Mo(001) surface which accompanies cesiation, as in the case of W(001),[4] occurs primarily above the plane of substrate surface atoms. This effect is due to the screening by the d electrons at the surface. In addition, cesiation leads to slight shifts of charge in the interior layers of the Mo film.

The work-function lowering for Cs/Mo at a Cs height of 2.9 Å is 2.01 eV, while for Cs/W (at the same height) the lowering is 2.35 eV. This difference in work-function lowering is evident in the slight differences of the planar-averaged Coulomb potentials shown in Figs. 11 and 12. These figures reveal that δV_c reaches 3 eV between W(S) and Cs, and only 2.7 eV for Cs/Mo. Furthermore, the average shift of the interstitial potential between central and subsurface atoms (cf. Figs. 11 and 12) is 2.0 eV for Cs/Mo and 2.2 eV for Cs/W. We attribute the smaller work-function change in the Cs/Mo system to the slightly greater polarizability of Mo compared with W as related to their surface electronic structure, in particular the relative locations of s and d states.

IV. SUMMARY AND CONCLUSION

The aim of this work was to deepen our theoretical understanding of interactions between alkali atoms and transition-metal surfaces. Using all-electron local-density-functional theory and the full-potential linearized augmented-plane-wave method, we have studied the electronic structure of a five-layer Mo(001) slab with $c(2\times2)$ overlayers of cesium atoms on both sides of the slab. The present study provides detailed insight into the cesium-induced effects on the two-dimensional energy-band structure; it deepens our understanding of the work-function lowering upon cesiation and it maps out the subtle differences between the system Cs/W(001) and Cs on Mo(001).

Similar to the case of the W(001) surface, we find that cesiation causes a shift to greater binding energies of the high-lying Mo d surface state located in the center of the two-dimensional BZ. This shift (of 0.9 eV) is caused by the formation of a polarized covalent bond between the d_{z^2} Mo d surface state and cesium s valence state. The shifted surface state retains its characteristic spatial extension as revealed by plots of single-particle charge densities; near the Cs nucleus these show the structure characteristic of a cesium 6s state. The energy-band structure shows that this Mo(d)-Cs(s)-like state at $\bar{\Sigma}$ is connected to a band with an upward dispersion away from $\bar{\Sigma}$ bar. This band, which can be considered as the remnant of a Cs valence band cuts the Fermi level about $\frac{1}{3}$ of the way between the center and the edge of the first BZ. The existence of this occupied band demonstrates that in the high-coverage limit, the Cs atoms are not ionized but rather show a metallic polarized behavior.

The existence of occupied Mo-Cs states at -0.2 eV provides evidence for covalent polarized Cs(d)—Mo(d) bonding. The energy-band structure shows that these states occur near the edge of the first BZ, near the symmetry point $\bar{X}'$. An unoccupied Cs(d)-Mo(d) state, particularly at 0.8 eV above the E_F, exists throughout the surface BZ.

These interactions between the Cs adsorbate and the Mo(001) substrate lead to a lowering of the high surface-local DOS at the E_F present on the clean Mo(001) surface. This high density of surface states and surface resonance states leads to a structural instability of the clean surface. In fact, both the W and the Mo surfaces are known to have reconstructed surfaces at low temperatures. Thus, the presence of alkali-metal atoms in fourfold-hollow sites found at half-monolayer coverage can be expected to inhibit reconstruction due to the lowering of the high density of states at the E_F.

Similar to the W(001) surface, the work-function lowering is explained by the formation of multiple surface dipoles. The major effect is a polarization of the Cs s-derived valence states towards the transition-metal surface leading to an increase of electronic charge between the Cs and the surface W atoms and a depletion of electronic charge outside the Cs, relative to the free, neutral Cs atoms. This dipole acts to decrease the work function. The occurrence of cesium p and d states in the occupied region of the valence bands, the bonding between Cs 5p semicore states and Mo sp-like valence states together with the counterpolarization of the inner parts of the Cs 5p states, lead to further modifications in the charge distributions in the surface and interface region and thus also influence the value of the work function.

Finally, the present work shows striking similarities between the Cs on W and Cs on Mo cases. Both systems show a similar shift of the high-lying surface state and virtually no shift for the low-lying state at $\bar{\Gamma}$. Furthermore, the Cs-induced charge redistribution leads to a similar work-function lowering. In conclusion, the detailed insight gained from the present study of Cs atoms adsorbed on the Mo(001) surface also provides a better understanding of the isoelectronic and isostructural system Cs on W(001).

ACKNOWLEDGMENTS

This work was supported by the Office of Naval Research (Grant No. N00014-81K-0438) and the Department of Energy. The excellent support of the National Magnetic Fusion Energy Computing Center is greatly appreciated.

---

*Present address: Naval Research Lab., Code 4684, Washington, D.C. 20375.

†Present address: Cray Research, Inc., 1333 Northland Drive, Mendota Heights, MN 55120.

[1]P. J. Schneider, K. H. Berkner, W. G. Graham, R. V. Pyle, and J. W. Stearns, Phys. Rev. B **23**, 941 (1981); J. R. Hiskes and P. J. Schneider, *ibid.* **23**, 949 (1981).

[2]M. Wada, R. V. Pyle, and J. S. Stearns, in *Production and Neutralization of Negative Ions and Beams, Proceedings of the 3rd International Symposium, Brookhaven, 1983,* AIP Conf. Proc.

No. 111, edited by K. Prelec (AIP, New York, 1984), p. 247.
[3]P. J. M. van Bommel, K. N. Leung, and K. W. Ehlers, in *Production and Neutralization of Negative Ions and Beams, Proceedings of the 3rd International Symposium, Brookhaven, 1983,* AIP Conf. Proc. No. 111, edited by K. Prelec (AIP, New York, 1984), p. 258; J. R. Hiskes, A. M. Karo, E. Wimmer, A. J. Freeman, and S. R. Chubb, J. Vac. Sci. Technol. A **2**, 670 (1984).
[4]E. Wimmer, A. J. Freeman, J. R. Hiskes, and A. M. Karo, Phys. Rev. B **28**, 3074 (1983); E. Wimmer, A. J. Freeman, M. Weinert, H. Krakauer, J. R. Hiskes, and A. M. Karo, Phys. Rev. Lett. **48**, 1128 (1982).
[5]P. Soukiassian, R. Riwan, C. Guillot, J. Lecante, and Y. Borensztein, Phys. Scr. **T4**, 110 (1983); R. Riwan, P. Soukiassian, C. Guillot, J. Lecante, and S. Zuber, Le Vide-les Couches Minces **38**, 125 (1983).
[6]P. Soukiassian, R. Riwan, J. Lecante, E. Wimmer, S. R. Chubb, and A. J. Freeman, Phys. Rev. B **31**, 4911 (1985).
[7]V. L. Moruzzi, J. F. Janak, and A. R. Williams, *Calculated Electronic Properties of Metals* (Pergamon, New York, 1978).
[8]H. J. F. Jansen and A. J. Freeman, Phys. Rev. B **30**, 561 (1984).
[9]J. E. Inglesfield, Vacuum **31**, 663 (1981), and references therein.
[10]R. Riwan, P. Soukiassian, S. Zuber, and J. Cousty (unpublished).
[11]V. B. Voronin, A. G. Naumovets, and A. G. Fedorus, Pis'ma, Zh. Eksp. Teor. Fiz. **15**, 523 (1972) [JETP Lett. **15**, 370 (1972)].
[12]P. Soukiassian, R. Riwan, and Y. Borensztein, Solid State Commun. **44**, 1375 (1982).
[13]C. A. Papageorgopoulos and J. M. Chen, Surf. Sci. **39**, 283 (1973).
[14]E. Wimmer, H. Krakauer, M. Weinert, and A. J. Freeman, Phys. Rev. B **24**, 864 (1981).
[15]M. Weinert, E. Wimmer, and A. J. Freeman, Phys. Rev. B **26**, 4571 (1982).
[16]Equation (3.58) of D. Pines, *Elementary Excitations in Solids* (Benjamin, New York, 1963), provides an expression for $E_{\rm corr}$, where $V=\partial(n\epsilon_{\rm corr})/\partial n-2(3/\pi n)^{1/3}$ is the effective, single-particle potential, measured in Ry.
[17]P. Hohenberg and W. Kohn, Phys. Rev. **136**, 864 (1964).
[18]W. Kohn and L. J. Sham, Phys. Rev. **140**, A1133 (1965).
[19]D. D. Koelling and B. N. Harmon, J. Phys. C **10**, 3107 (1977).
[20]C. S. Wang and A. J. Freeman, Phys. Rev. B **19**, 793 (1977).
[21]M. Weinert, J. Math. Phys. (N.Y.) **22**, 2433 (1981); also, see Ref. 14.
[22]D. G. Anderson, J. Assoc. Comput. Mach. **12**, 547 (1965); D. R. Hamann (private communication).
[23]Shang-Lin Weng, T. Gustafsson, and E. W. Plummer, Phys. Rev. Lett. **39**, 822 (1977).
[24]G P. Kerker, K. M. Ho, and M. L. Cohen, Phys. Rev. Lett. **40**, 1593 (1978).
[25]E. Wimmer, J. Phys. F **13**, 2313 (1983).
[26]S. R. Chubb (unpublished).